

## PUBLISHED VERSION

Manpreet Singh, M.S. Mohamed Ali, Abdul H Sheikh, Michael Griffith and Phillip Visintin  
**Structural behaviour of ultra high performance fibre reinforced concrete beams with steel and polymer bar reinforcement**

Proceedings of The 11th fib International PhD Symposium in Civil Engineering, 2016 /  
Maekawa, K., Kasuga, A., Yamazaki, J. (ed./s), pp.287-294.

This publication is available on Internet under the following Creative Commons license.  
Some rights reserved. Published: <http://creativecommons.org/licenses/by-nc-nd/4.0/>

Published publication available at: [http://concrete.t.u-tokyo.ac.jp/fib\\_PhD2016/](http://concrete.t.u-tokyo.ac.jp/fib_PhD2016/)

### PERMISSIONS

<http://creativecommons.org/licenses/by-nc-nd/4.0/>



Attribution-NonCommercial-NoDerivatives 4.0 International (CC BY-NC-ND 4.0)

This is a human-readable summary of (and not a substitute for) the [license](#).

[Disclaimer](#)

#### You are free to:

**Share** — copy and redistribute the material in any medium or format

The licensor cannot revoke these freedoms as long as you follow the license terms.

#### Under the following terms:



**Attribution** — You must give **appropriate credit**, provide a link to the license, and **indicate if changes were made**. You may do so in any reasonable manner, but not in any way that suggests the licensor endorses you or your use.



**NonCommercial** — You may not use the material for **commercial purposes**.



**NoDerivatives** — If you **remix, transform, or build upon** the material, you may not distribute the modified material.

**No additional restrictions** — You may not apply legal terms or **technological measures** that legally restrict others from doing anything the license permits.

26 October 2016

<http://hdl.handle.net/2440/101999>

# Structural behaviour of ultra high performance fibre reinforced concrete beams with steel and polymer bar reinforcement

Manpreet Singh, M.S. Mohamed Ali, Abdul H Sheikh, Michael Griffith and Phillip Visintin

*The University of Adelaide,  
North Terrace, Adelaide, S.A., Australia*

## Abstract

In this study, ultra high performance fibre reinforced concrete (UHPFRC) beams with internal bar reinforcement are tested. The objective is to investigate the flexure behaviour of developed UHPFRC material in full scale structural members. Five full scale beams of 3.25m span, reinforced with different reinforcing materials are tested under four point bending. The flexural capacities, load displacement behaviour, cracking and failure pattern is obtained from the test results. The beams with steel reinforcement exhibited ductile failure. The fibres effectively resisted the opening of the cracks. The ultimate failure of beams is due to the rupture of reinforcing bars. The numerical models are developed for the tested beams for which concrete damaged plasticity model is adopted to simulate the material behaviour of UHPFRC. The material parameters required for the constitutive model is identified by conducting material tests under tension and compression. The developed numerical models are validated with the experimental results obtained from full-scale beam tests. The results obtained from the developed numerical models are in good agreement with the experimental data.

## 1 Introduction

The excellent mechanical properties of ultra high performance fibre reinforced concrete (UHPFRC) make it a suitable material for the construction of taller, longer, durable and sustainable structures. In recent years, the use of UHPFRC in construction of bridges, lightweight structures and retrofitting of structures has increased significantly. UHPFRC is generally characterized as the reactive powder concrete with compressive strength exceeding 150MPa containing sufficient fibre content to achieve strain hardening under tension (AFGC 2002, Graybeal 2005). Several proprietary mixes are developed such as SIFCON, Ductal, CARDIFRC and CEMTEC and has been used in construction applications. The tensile characteristics of the material enables to design innovative structures without using conventional steel bar reinforcement (Voo et al. 2012). The elimination of reinforcement reduces weight of the structure and speeds construction process (Ferrier et al. 2015).

In past few years, the new type of reinforcing materials in the form of fibre reinforced polymer (FRP) bars emerged as an effective way of enhance the corrosion resistant of structures. The replacement of steel bars with FRP material is found to have advantages such as high corrosion resistance, high strength to weight ratio, non conductivity and ease of handling (Ehsani et al. 1997). The use of FRP bars with UHPFRC can provide a new way of optimizing the structural members. The objective of this research is to investigate the flexural behaviour of UHPFRC beams reinforced with different materials such as glass FRP bars, carbon FRP bars, high strength steel tendons and conventional steel bars. The load displacement behaviour, cracking pattern and failure modes of the beams developed with different rebar material is compared. The non linear finite element analysis is conducted for all the tested beams.

## 2 Experimental program

### 2.1 Test specimens

To investigate the flexural behaviour of UHPFRC beams reinforced with different rebar material, 5 full-scale beams are tested. The beams are manufactured with UHPFRC mix developed at the University of Adelaide. The details of all the test beams are given in Table 1. All the beams are of 250 x

250mm cross-section with a span of 3250mm. The beams are designated with a first letter as “B” representing the specimen is a beam followed by a letter representing the name of the rebar material used and then followed a number representing the diameter of rebar used as tensile reinforcement. The letter “S”, “G”, “C” and “T”, represents the reinforcing bar material as steel bar, glass FRP (GFRP) bar, carbon FRP (CFRP) bar and low relaxation strands (LRS) respectively. For example the beam with steel rebar of 20mm diameter is designated as BS20. To assure the flexure failure mode of the beam, the shear reinforcement is also provided which consisted of 8mm diameter stirrups spaced at 90mm centre to centre up to the load points. The zone between the load points is not provided with the stirrups to eliminate the confinement of concrete with stirrups.

Table 1 Detail of beam specimens

Beam	Dimension B x D (mm)	Reinforcing material	Bar diameter (mm)	Number of bars	Reinforcement percentage
BS20	250 x 250	Steel	20	3	1.5%
BS25	250 x 250	Steel	25	3	2.4%
BG20	250 x 250	GFRP	20	3	1.5%
BC12	250 x 250	CFRP	12	3	0.5%
BT15	250 x 250	LRS	15.2	3	0.9%

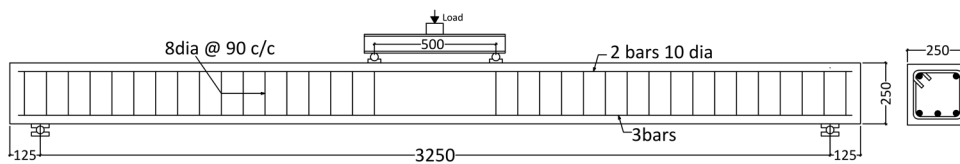


Fig. 1 Detail of beam specimens.

## 2.2 UHPFRC mix

The UHPFRC used in this investigation is developed at The University of Adelaide using locally available conventional raw materials the details of which can be found in (Sobuz et al. 2016). The proportioning of material for the UHPFRC mix adopted in this study is given in Table 2. The constituents of mix include the binder consisting of sulphate resistant cement and silica fume. The river washed sand from local quarry is used as filler and no coarse aggregates are used. The water to binder ratio is 0.1775 and third generation liquid based High range water reducing admixture (HRWR) of Sika Viscocrete is used. The steel fibres used are hooked end steel fibres of 35mm in length with aspect ratio of 64 and yield strength of 1100MPa reported by the manufacturer. The amount steel fibre added is 2.25% by volume.

All the dry constituents are electronically weighed and mixed in dry state in horizontal pan mixer for at least 3 minutes. The water and HRWR are mixed together and added into the material and allowed to mix until the materials turns into a flow-able consistent paste. The steel fibres are then added and mixed for further 5 minutes.

Table 2 UHPFRC mix details

Cement	Sand	Silica Fume	HRWR	Water	Steel Fibre
1	1	0.266	0.045	0.1775	2.25% by Vol

## 2.3 Material properties

### 2.3.1 UHPFRC properties

The cylindrical specimens of 100mm diameter and 200mm height are used to obtain the compressive stress strain curve of the developed UHPFRC mix. The cylindrical specimens are casted from each

batch and tested for compressive strength at 28 days and on the day of the beam test as well. The elastic modulus of the UHPFRC obtained from the cylinder test is 38GPa. Figure 2 (left) shows the typical compressive stress strain curve of the UHPFRC obtained from the tests.

The uniaxial tensile test set up is developed to determine the tensile properties of the material for which a dog bone shaped specimen of 120mm x 120mm cross section as shown in figure 2(middle) is fabricated. The sides of the specimen are clamped between the specially designed test set up which is then attached to the instron machine. The displacement controlled loading is applied at the rate of 0.01mm/min for whole test. Figure 2(right) shows the typical tensile behaviour of the UHPFRC obtained from the dog bone test specimen.

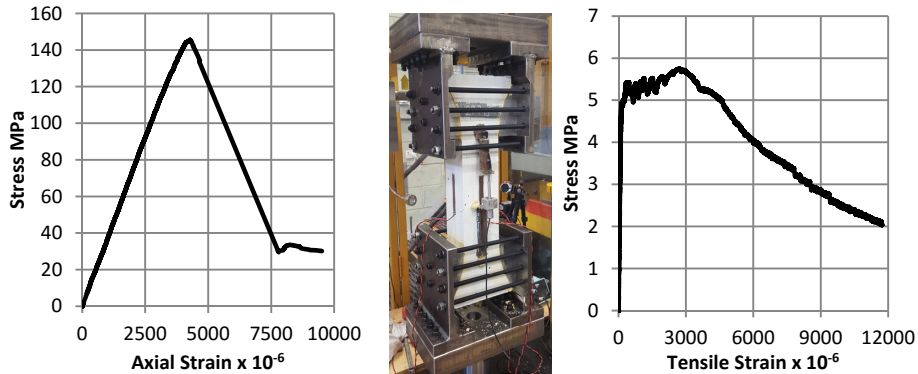


Fig. 2 Compressive stress strain (Left), Tensile test set up (middle), Tensile stress strain (right)

### 2.3.2 Reinforcing bar properties

The deformed steel bars used as reinforcement has nominal yield strength of 500MPa and ultimate tensile strength of 625MPa. The coupon test performed for steel bars only. The high modulus glass FRP bars used has a elastic modulus of 62GPa with tensile strength of 1100MPa whereas carbon FRP has the values of 144GPa and 1800MPa respectively, reported by the manufacturer. The detail properties of all the reinforcing material used are shown in table 3.

Table 3 Reinforcing bars properties

Material	Elastic Modulus GPa	Tensile Strength MPa	Rupture strain %
Steel	195	500	15
GFRP	62	1100	1.73
CFRP	144	1800	1.32
LRS	195	1750	3.5

## 2.4 Fabrication of beams

The beams are fabricated one at a time due to the large amount of material required. The horizontal mixer of 1 ton capacity installed at The University of Adelaide is used for the onsite manufacturing of the structural members. The wooden formwork is built for the casting of the beams and all the beams are casted horizontally. The specimens required for the material tests are also casted for each batch of concrete. After 2 hours of casting all the specimens are covered with wet hessian and plastic sheets for at least 24hours. The formwork is then removed and the beams are cured with wet hessian covered with plastic sheets for at least 28 days before testing.

## 2.5 Test setup and procedure

The beams are subjected to two equal concentrated loads applied symmetrically at a distance of 250mm from the mid span, so as to induce pure bending stresses in the beam between the load points. The load is applied through a single hydraulically actuated jack to the steel section placed on the top

face of the beam with its supports 500mm apart. The beams are tested until collapse with monotonically applied load and the corresponding deflections and strains are recorded simultaneously.

### 3 Experimental results

#### 3.1 Load-deflection relation

The deflection is measured at mid span for all the beams. Figure 3 and 4 shows the load versus mid span displacement relationship obtained from the tests. The load-displacement curves indicate that the relation can be divided into three to four distinct regions, namely initial linear zone before first cracking, yield load at the yielding of rebar, peak load and collapse load of beam. The first stage of load displacement curve corresponds to the high bending stiffness of the uncracked section response of the beams. The first cracking load for beams is BS20, BS25 is 20kN and for beams BG20 and BC12 is 26kN, whereas the lowest recorded first cracking load of 10kN is obtained for beam reinforced with low relaxation strand BT15. After the first cracking load, the reduction in bending stiffness is observed due to the initiation of microcracks. The load displacement curve observed to be linear with reduced stiffness until the yield load is attained. The reduction in stiffness is found to be dependent on the stiffness provided by the reinforcing bar material that is a factor of elastic modulus of bars, percentage of reinforcement provided and bond slip relation.

The failure of beams BS20, BS25, BC12 and BT15 initiated due to the yielding of the reinforcing bars, whereas beam BG20 yielded due to the crushing of concrete. The beams with steel bars (BS20, BS25) and low relaxation strands (BT15) is found to have long ductile plateau after the yield load is attained with the final collapse is due to the rupture of the reinforcing bars. The beam BC12 with CFRP rebar observed to have negligible ductility after the yield load and the beam failed in a sudden manner due to rupture of CFRP bars. The failure of beam BG20 initiated with the crushing of concrete. Although the beam has less ductility, the load drop is gradual as the crushing of UHPFRC is progressed which is different to the sudden and brittle failure observed for cylindrical specimens under pure compression.

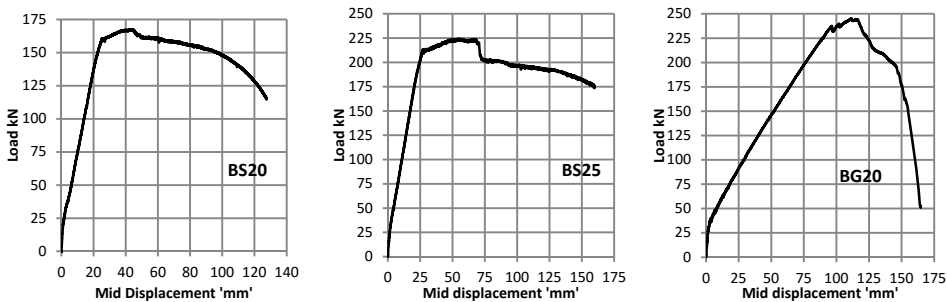


Fig. 3 Load displacement of beam BS20(Left), BS25(middle), BG20(right)

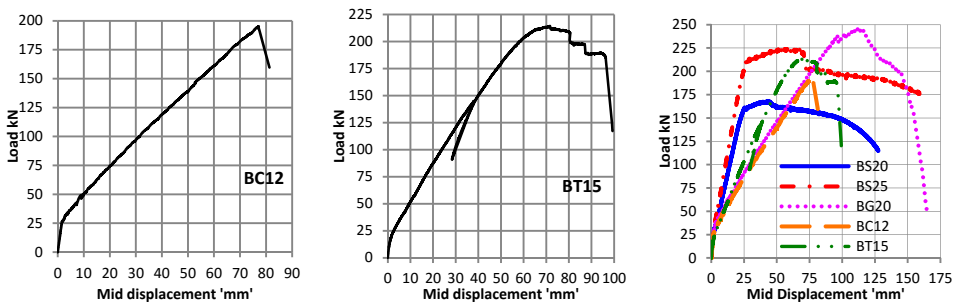


Fig. 4 Load displacement of beam BC12(Left), BT15(middle), Load displacement of all beams(right)

### 3.2 Cracking and failure pattern

At first cracking load there is no visible cracks are observed. After first cracking as described earlier the slope of the load deflection curve became less steep comparing to initial slope, indicates the formation of micro-cracks, although no visible cracks are observed. With further increase in load, the widely spaced hairline cracks became visible throughout the beams. The number of cracks increased with the increase of load and new cracks developed between the existing ones. The cracks propagated vertically towards the compression face of the beam. At yield load the crack width of one or two cracks became significantly greater than the other cracks. The steel fibres resisted the opening of the cracks allowing the beam to take further load. At peak load on of the crack in constant moment zone (between the load points) propagated throughout the depth of the beam that formed a hinge. With further applied displacement the fibres kept pulled out and load dropped gradually. The beams with tension failure mode finally collapsed due to the rupture of reinforcement bars. The failure pattern indicated that the fibres effectively resisted the opening of cracks that lead to the increased load carrying capacity even after the reinforcement is yielded. The compression failure mode is observed only for BG20 for which the cracking pattern is found to be similar as observed for beams with tension failure mode with the exception that the crack is only propagated upto the one third depth of the beam.

Table 4 summarises the experimental results obtained from the beam tests. The tested beams indicate that tension failure mode remains up to the reinforcement percentage of 2.4% for conventional steel rebars. The results also indicate that only 1.5% of reinforcement is required for high modulus GFRP material to obtain the compression failure mode of the beams. The beam BC12 with only 0.5% of reinforcement attained the similar stiffness as of beam BG20 with 1.5% of reinforcement. The load carrying capacity of BC12 is found to be 18% greater than BS20 which has 3 times reinforcement percentage when compared to BC12.

Table 4 Summary of results

Beam	Cracking Load kN	Cracking Disp. 'mm'	Yield Load kN	Yield Disp. 'mm'	Ultimate Disp. 'mm'	Failure Mode
BS20	20	1.0	161	25	128	Tension
BS25	20	1.0	206	26	158	Tension
BG20	26	1.5	234	94	143	Compression
BC12	26	1.6	191	75	81	Tension
BT15	10	0.5	209	64	95	Tension

## 4 Numerical modelling

The numerical modelling of the beams is done with non-linear finite element analysis. The concrete damaged plasticity (CDP) constitutive model is used to model the behaviour of UHPFRC material. The CDP model uses the failure criterion proposed by (Lubliner et al. 1989) and incorporates the modifications proposed by (Lee and Fenves 1998) to account for different evolution of strength under tension and compression. The material properties are extracted from the experimental tests, as explained in earlier sections, served as input for CDP model. The other parameters required to define the CDP model are given in table 5.

Table 5 Parameters of CDP Model

Parameter	Value
Dilation Angle	35
Eccentricity	0.1
$\sigma_{b0}/\sigma_{c0}$	1.05
Kc	2/3
Viscosity parameter	0.005

Figure 5a shows the typical finite element model of beam. The beams are modelled as 3D solid deformable parts meshed with 8 node reduced integration brick elements (C3D8R). The reinforcement is modelled as 3D deformable wire part and meshed as two node 3D truss elements (T3D2). The reinforcement is embedded in the solid element of the concrete beam by using the built in embedment constraint with default values, hence full bond between reinforcement and concrete is assumed. The supports are modelled as 3D solid deformable steel elements of 50mm square cross section with pinned boundary condition applied at the middle partition line. The interaction between beam and support is provided as surface to surface standard contact with hard interaction property and frictional coefficient of 0.1 is also defined. The displacement type boundary condition is applied at the load points. The effect of mesh refinement on the numerical results is tested by analysing a beam with different element sizes such as 50mm, 25mm and 15mm so as to ensure the convergence of results. The mesh with 25mm element size successfully predicted the overall load displacement behaviour. The further reduction in the element size increased the computational time significantly without showing any visible improvement of the results. Based on these observations, an element size of 25mm is adopted for modelling all the beams. The reaction forces, mid span displacement and other variables are extracted as history output for each step increment to compare the results.

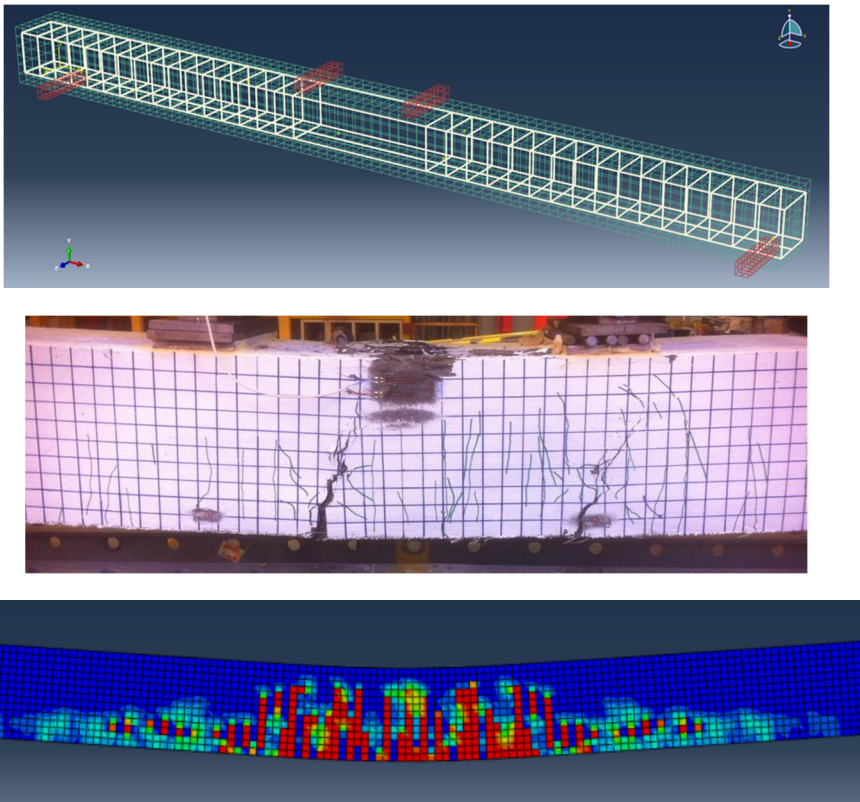


Fig. 5 Finite element model of beam (top), Typical cracking pattern of tested beam (middle), Tensile damage contours obtained from finite element model of beam (bottom).

#### 4.1 Comparison of results

Figure 5 shows that the cracking pattern captured by the numerical model is similar to that found in the actual test. Figure 6 and 7 compares the load deflection behaviour obtained from the finite element analysis of the beams with the experimental results. The simulations accurately meet the global load displacement relation of the tested beams. The initial stiffness of the beams in the rising branch of load displacement curve is slightly overestimated by the simulations. The yield load is also slightly overestimated by numerical simulation by 3% to 10%. The numerical results by (Yoo and Yoon 2015) also overestimated the stiffness of rising branch and load carrying capacity by 18% in beams with similar geometry of fibres (with coefficient of fibre orientation as 1). The inverse analysis of

prism data is adopted by (Yoo and Yoon 2015) to extract the tensile behaviour of UHPFRC. However in this study the tensile behaviour of UHPFRC is extracted from the direct tensile test and used for the numerical simulations. The numerically obtained results in present study by using the tensile properties obtained from direct tensile test has shown the reduced error in the predictions of load carrying capacities of reinforced UHPFRC beams. The slight overestimation of the predictions indicates that the dispersion, orientation of fibres is disturbed due to the presence of longitudinal reinforcement and shear stirrups. Table 6 compares the results obtained from numerical simulations with experimental data.

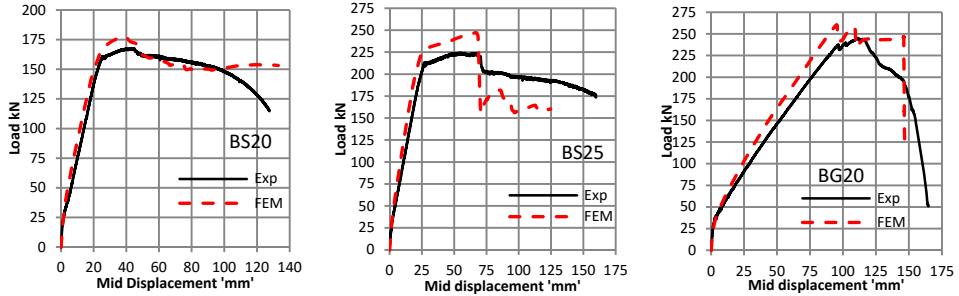


Fig. 6 Comparison of experimental and numerical results of beams BS20(left), BS25(middle), BG20(right)

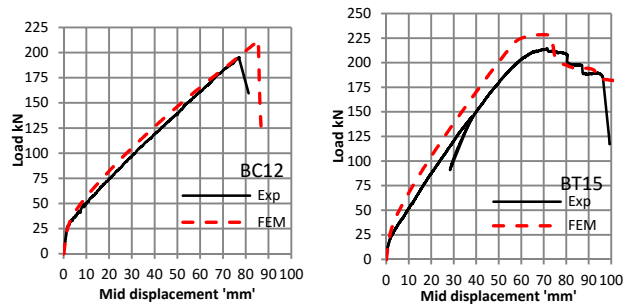


Fig. 7 Comparison of experimental and numerical results of beams BC12(left), BT15(right)

Table 6 Comparison of experimental and numerical results

Beam	Yield Load $P_{Exp}$ (kN)	Yield disp. $\Delta_{Exp}$ (mm)	Yield Load $P_{FEM}$ (kN)	Yield disp. $\Delta_{FEM}$ (mm)	$P_{Exp}/P_{FEM}$
BS20	161	25	166	26	0.97
BS25	206	26	228	28	0.90
BG20	234	94	250	96	0.94
BC12	191	75	207	86	0.93
BT15	209	64	222	58	0.94

## 5 Conclusions

This paper presents the results of experimental investigation on the flexural behaviour UHPFRC beams reinforced with different reinforcing materials. The numerical model is developed and is validated with the results obtained from the experimental data. The following conclusions are drawn from the test and numerical results:

The UHPFRC beams reinforced with conventional steel rebars exhibit very ductile failure. The fibres resisted the opening of the cracks and contributed toward the increased load carrying capacity



of beams even after the steel bars are yielded. The tension mode of failure is observed up to 2.4% percentage of steel reinforcement. Whereas, the beam with high modulus GFRP rebars found to have compression failure mode with 1.5% of reinforcement.

The beams reinforced with FRP materials has reduced stiffness when compared with beams with steel rebars, however the cracking pattern is observed to be similar for both type of reinforcing materials. The beam with 0.5% of CFRP reinforcement has tension mode of failure whereas the stiffness achieved is identical to the beam with 1.5% of GFRP reinforcement and 18% greater load capacity than beam with 1.5% of steel reinforcement. Further tests are required to obtain the percentage of CFRP reinforcement required to change the mode of failure from tension to compression.

The concrete damaged plasticity model is found reliable to simulate the material behaviour of UHPFRC when provided with the input properties of tension and compression response of UHPFRC obtained from experimental results. The numerical models developed for the beams accurately load displacement behaviour under flexure loading. The ratio of flexural capacity of beams obtained from experimental to numerical results is in range of 0.90 to 0.97, shows that the numerical results are in good agreement with the experimental data. The developed numerical model will be used for further parametric study of beams. The parameters varied will be percentage of tensile reinforcement, shear reinforcement, span and cross section of beams.

### Acknowledgements

The authors wish to acknowledge the financial support of the Australian Government Department of Defence's "Defence Science and Technology Organisation".

### References

- AFGC. 2002, Interim recommendations for Ultra high performance fibre reinforced concrete.
- Ehsani M.R., Saadatmanesh H. and Tao S., 1997 "Bond behaviour of GFRP rebars". *Journal of Composite Material* 31(14): 1413–1430.
- Ferrier E., Michel L., Zuber B. and Chanvillard G., 2015 "Mechanical behaviour of ultra high performance short fibre reinforced concrete with internal fibre reinforced polymer bars." *Composites-PartB* 68:246-258
- Graybeal, Benjamin A. 2005 "Characterization of the behaviour of ultra high performance concrete", PhD diss, University of Maryland.
- Lee J., and Fenves G.L., 1998 "Plastic-Damage Model for Cyclic Loading of Concrete structures" *Journal of Engineering Mechanics*, 124- 8:892–900.
- Lubliner J., Oliver J., Oller S., and Oñate E, 1989 "A Plastic-Damage Model for Concrete," *International Journal of Solids and Structures* 25:299–329
- Sobuz H.R., Visintin P., Mohamed Ali M.S., Singh M., Griffith M.C. and Sheikh A.H., 2016 "Manufacturing Ultra-High Performance Concrete Utilising Conventional Materials and Production Methods" *Construction and Building materials* 111:251-261.
- Voo Y.L., Nematollahi B., Said A.B.B.M, Gopal B.A. and Yee T.S., 2012. "Application of Ultra High Performance Fibre Reinforced Concrete- The Malaysia Perspective". *International Journal of Sustainable Construction Engineering & Technology* 3-1:26-44
- Yoo D.Y., Yoon Y.S., 2015 "Structural performance of ultra high performance concrete beams with different steel fibres", *Engineering Structures* 102:409-423.